Syntheses, Structures and Spectroscopic Properties of Mixed-Ligand Chromium(III) Complexes Containing 1,2-Bis(dimethylphosphino)ethane, 1,3-Bis(dimethylphosphino)propane or 1,1,1-Tris(dimethylphosphinomethyl)ethane

Takayoshi Suzuki,* Kazuo Kashiwabara,† Tsutomu Usami,† Takeshi Imamura, Masakazu Kiki, Junnosuke Fujita,† and Sumio Kaizaki

Department of Chemistry, Graduate School of Science, Osaka University, Toyonaka 560-0043

†Department of Chemistry, Graduate School of Science, Nagoya University, Nagoya 464-8602

(Received December 13, 2000)

Mixed-ligand chromium(III) complexes containing di- or tridentate phosphines, *trans*-$[CrX_2(dmpe)_2]^+$ (X = Cl, Br, I, CN, NCS or N_3; dmpe = $Me_2P(CH_2)_2PMe_2$), *trans*-$[CrX'_2(dmpp)_2]^+$ (X′ = Cl, Br or I; dmpp = $Me_2P(CH_2)_3PMe_2$), $[CrX''_3(tdmme)]$ (X″ = Cl, Br, CN or NCS; tdmme = $MeC(CH_2PMe_2)_3$) and $[CrCl_2(tdmme)(PMe_3)]^+$, have been prepared and their structures and spectroscopic properties have been investigated. The single-crystal X-ray analyses of *trans*-$[CrI_2(dmpp)_2]I$ (**6**) and $[Cr(CN)_3(tdmme)]\cdot 2H_2O$ (**16**$\cdot 2H_2O$) have also been reported. The Cr–P bond length in **6** (2.5147(6) Å) is longer than those in *trans*-$[CrCl_2(dmpe)_2]BPh_4$ (av 2.445 Å) and in **16**$\cdot 2H_2O$ (av 2.455 Å). In the UV-vis absorption spectra of *trans*-$[Cr(Cl\ or\ Br)_2(dmpe\ or\ dmpp)_2]^+$, an intense ($\varepsilon > 1000$ $dm^3\ mol^{-1}\ cm^{-1}$) absorption envelope is observed at 20000–30000 cm^{-1}, in addition to the $^4B_1 \rightarrow a^4E$ d–d transition band at ~17000 cm^{-1} (ε = 44–65 $dm^3\ mol^{-1}\ cm^{-1}$). The envelope consists of three d–d transition components: $^4B_1 \rightarrow {}^4A_2$, $^4B_2$ and b^4E, similar to the corresponding $H_2N(CH_2)_2NH_2$ (= en) complexes. The magnetic circular dichroism (MCD) spectra of these didentate phosphine complexes show a spin-forbidden d–d transition ($^4B_1 \rightarrow {}^2E, {}^2B_2$) component at ~19000 cm^{-1}. The ligand-field and Racah parameters, $\Delta(d)$, $\Delta(e)$, $\Delta(t_2)$ and B, of the complexes are estimated. It is found that the ligand-field and repulsion parameters of the dmpp complexes are almost the same as those of the corresponding en complexes. For the dmpe complexes, while $\Delta(d)$ is just slightly smaller than those of the dmpp and en complexes, the tetragonal symmetry parameters, $\Delta(e)$ and $\Delta(t_2)$, are much reduced. The ligand-field perturbation energies of phosphines are estimated as $\Delta_{dmpp} = 21830 > \Delta_{tdmme} = 20920 > \Delta_{dmpe} = 20620$ cm^{-1}, the order of which is strange, since the Cr–P bond lengths in the complexes *increase* in the order of dmpp > tdmme > dmpe. Furthermore, the interelectronic repulsion parameter B of $[Cr(Cl\ or\ Br)_3(tdmme)]$ estimated from the $^4A_2 \rightarrow {}^4T_1$ transition energy (B_{35}) is remarkably much smaller than the parameter estimated from the spin-forbidden $^4A_2 \rightarrow {}^2T_2$ transition energy (B_{55}).

In contrast to the extensive work on chromium(III) complexes formed with hard Lewis bases such as am(m)ines and oxygen-donor ligands,[1] relatively few investigations have been carried out for chromium(III) complexes containing phosphines or arsines, which are known as soft Lewis bases. Before 1980, only *trans*-$[Cr(Cl\ or\ Br)_2(diphos\ or\ diars)_2]ClO_4$ (diphos = *o*-$C_6H_4(PMe_2)_2$;[2] diars = *o*-$C_6H_4(AsMe_2)_2$[3]) had received more than cursory studies on syntheses and spectroscopy of chromium(III)-phosphine or arsine complexes. In 1983–1984, Levason et al. described[4,5] such complexes having di-, tri-, or tetradentate phosphines or arsines: $Ph_2P(CH_2)_2PPh_2$, *cis*-$Ph_2PCH{=}CHPPh_2$, $Me_2P(CH_2)_2PMe_2$ (dmpe), $PhP(CH_2CH_2PPh_2)_2$, $P(CH_2CH_2PPh_2)_3$ and $MeC(CH_2PPh_2)_3$. After 1985, several research groups reported synthesis and structural characterization of chromium(III) complexes with trialkylphosphines and di- or tridentate phosphines bearing dimethyl- or diethylphosphino groups: for example, *trans*-$[Cr(Cl\ or\ I)_2(dmpe)_2]^+$,[6] $[\{CrCl_3(dmpe)\}_2(\mu\text{-}dmpe)]$,[7] $[CrCl_4(PMe_3)_2]^-$,[8] $[Cr_2Cl_6(PMe_3\ or\ PEt_3)_4]$,[9] $[Cr_2Cl_6(Me_2PCH_2PMe_2)_2]$,[9] $[Cr_2Cl_6\{(Et_2PCH_2CH_2)_2PCH_2P(CH_2CH_2PEt_2)_2\}]$,[10] $[CrCl_3(tdmme)]$ (tdmme = $MeC(CH_2PMe_2)_3$),[11] $[Cr(Bu^n)_2Cl(tdmme)]$,[12] and $[Cr(Me)_3\{Bu^tSi(CH_2PMe_2)_3\}]$.[13] However, to our best knowledge, there are no systematic studies on chromium(III)–phosphine complexes to date. In particular, the spectroscopic properties and the ligand-field parameters of phosphines in the chromium(III) complexes are rarely reported, as compared to the extensive and detailed studies concerning those of the am(m)ine complexes.[1,14,15] We have, for a long time, carried out systematic studies on syntheses, structural and spectroscopic characterization of cobalt(III) complexes with di- or tridentate phosphines bearing dimethylphosphino groups.[16–22] As an extension of our synthetic efforts on phosphine complexes, it would be, therefore, challenging to study the analogous series of chromium(III) complexes.

In this paper, we will describe the preparation, structural characterization and spectroscopic properties of *trans*-$[CrX_2(dmpe\ or\ dmpp)_2]^+$-type (dmpp = $Me_2P(CH_2)_3PMe_2$; X = halide or pseudohalide ion) complexes, together with those

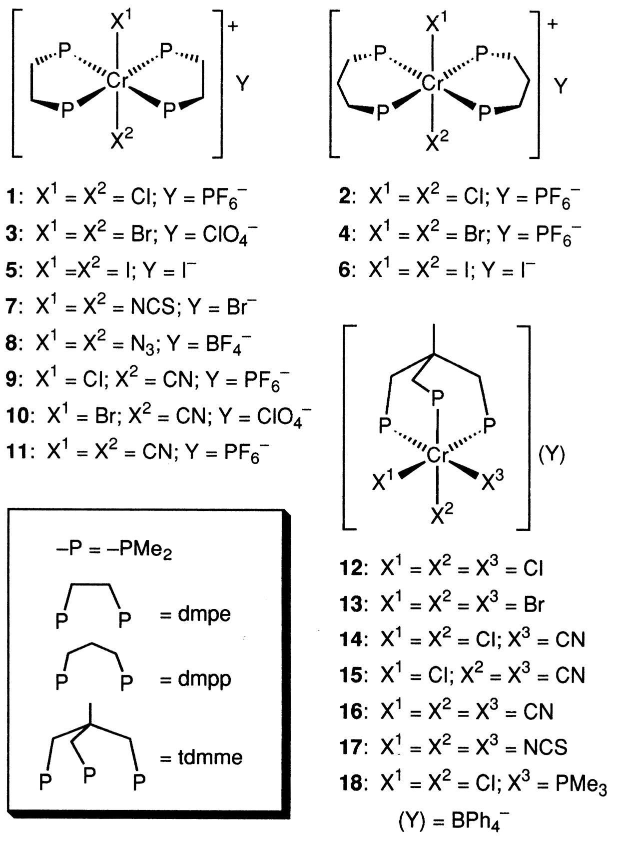

Scheme 1.

of $[CrX_3(tdmme)]$ and $[CrCl_2(tdmme)(PMe_3)]^+$ (Scheme 1). Among the complexes dealt with in this study, the syntheses and structural characterization of *trans*-$[CrCl_2(dmpe)_2]^+$,[6] *trans*-$[CrI_2(dmpe)_2]^+$,[6] and $[CrCl_3(tdmme)]$[11] have already been reported, but their absorption spectra have not been mentioned so far.

Experimental

General Remarks. The phosphines dmpe,[23] dmpp[24] and tdmme[25] were prepared according to literature methods, and were handled under a dinitrogen atmosphere using Schlenk techniques until they formed air-stable chromium(III) complexes. All of the solvents used in the preparation of the phosphines and their complexes were deaerated with dinitrogen for 20 min immediately before use. The starting complexes of $[CrBr_2(H_2O)_2(en)]Br$ (en = $H_2N(CH_2)_2NH_2$),[26] $[CrCl_3(tdmme)]$ (**12**)[11] and $[Cr(CO)_3(tdmme)]$[27] were prepared by the literature methods. Infrared spectra were measured on a Jasco IR A-3 or Shimadzu IR-435 spectrophotometer by the Nujol-mull method, UV-vis absorption spectra on a Hitachi 323 or a Perkin-Elmer Lambda 19 spectrophotometer, and MCD spectra on a Jasco J720 spectropolarimeter in a magnetic field of 1.5 T at room temperature.

***trans*-$[CrCl_2(dmpe)_2]PF_6$ (1).** A mixture of $CrCl_3\cdot6H_2O$ (610 mg, 2.29 mmol) and *N*,*N*-dimethylformamide (5 cm^3) was heated at 150 °C for 10 h, and then cooled to room temperature. To the resulting solution was added dmpe (681 mg, 4.58 mmol) dropwise with stirring; the mixture was stirred for 8 h at room temperature. Diethyl ether (200 cm^3) was added, affording a yellow-green oily product. After removal of the ethereal layer, excess $NaPF_6$ was added to the oily product, giving a green solid. It was dissolved in methanol, and the filtered solution was concentrated gradually in a desiccator to deposit green crystals. Yield: 752 mg (58%). Found: C, 25.78; H, 5.58%. Calcd for $C_{12}H_{32}Cl_2CrF_6P_5$: C, 25.36; H, 5.68%.

***trans*-$[CrCl_2(dmpp)_2]PF_6$ (2).** A mixture of anhydrous $CrCl_3$ (233 mg, 1.47 mmol) and dmpp (484 mg, 2.95 mmol) was heated at 140 °C for 30 min. After the reaction mixture was cooled to room temperature, 2-methoxyethanol (0.5 cm^3) was added, and the mixture was stirred overnight. The resulting oily product was dissolved in methanol (20 cm^3), and then filtered to remove unreacted $CrCl_3$. The filtrate was evaporated to a small volume under reduced pressure, and excess $NaPF_6$ was added to give a green precipitate. The precipitate was recrystallized from aqueous (75%) acetonitrile. Yield: 91 mg (10%). Found: C, 28.55; H, 6.23%. Calcd for $C_{14}H_{36}C_{12}CrF_6P_5$: C, 28.20; H, 6.09%.

***trans*-$[CrBr_2(dmpe)_2]ClO_4$ (3) and *trans*-$[CrBr_2(dmpp)_2]PF_6$ (4).** These complexes were prepared by methods similar to those of **1** and **2**, respectively, using $[CrBr_2(H_2O)_2(en)]Br$ as a starting Cr(III) material. For **3**, the following modifications were made to achieve the higher yield and better crystallinity: a higher reaction temperature (50 °C) with shorter reaction time (30 min) applied after the addition of dmpe, and crystallization with an aqueous $LiClO_4$ solution. The crude product obtained was recrystallized from aqueous (75%) methanol to give green crystals of the ClO_4^- salt (40%). Found: C, 23.51; H, 5.13%. Calcd for $C_{12}H_{32}Br_2ClCrO_4P_4$: C, 23.57; H, 5.27%. For **4**, recrystallization from a mixture of ethanol and acetonitrile (1 : 1) gave green crystals of the PF_6^- salt (34%). Found: C, 25.29; H, 5.21%. Calcd for $C_{14}H_{36}Br_2CrF_6P_5$: C, 24.54; H, 5.30%.

***trans*-$[CrI_2(dmpe)_2]I$ (5) and *trans*-$[CrI_2(dmpp)_2]I$ (6).** In a 100 cm^3 Schlenk tube, a 1-propanol solution (12 cm^3) of $CrI_3\cdot6H_2O$ (602 mg, 1.11 mmol) was gently heated to boil in the open air until the mixture became an oil by evaporation of the solvent. The Schlenk tube containing the resulting oil was purged with dinitrogen, and dmpe or dmpp (2.22 mmol) was added to give a greenish oil. The mixture was stirred for 10 min. The solidified product was washed with a small amount of diethyl ether, and recrystallized from methanol. **5**: yellow-green crystals (80%). Found: C, 20.10; H, 4.45%. Calcd for $C_{12}H_{32}CrI_3P_4$: C, 19.66; H, 4.40%. **6**: yellow-green crystals (85%). Found: C, 21.89; H, 4.70%. Calcd for $C_{14}H_{36}CrI_3P_4$: C, 22.10; H, 4.77%.

***trans*-$[Cr(NCS)_2(dmpe)_2]Br\cdot2H_2O$ (7·2H₂O).** To a methanol solution (40 cm^3) of **1** (150 mg, 0.26 mmol) were added NH_4NCS (100 mg, 1.32 mmol) and zinc (300 mg). The mixture was stirred for 30 min, and then filtered. The orange filtrate was diluted with water (3 dm^3) and applied on a column (ϕ 1.5 × 100 cm) of SP-Sephadex C-25 (Na^+ form). The adsorbed products were eluted with a 0.03 mol dm^{-3} aqueous NaBr solution, yielding a major orange and a minor yellow-green band. The orange eluate was concentrated to a volume of one-third under reduced pressure, and stored in a desiccator to give orange crystals. Yield: 17 mg (11%). Found: C, 28.22; H, 6.22; N, 4.62%. Calcd for $C_{14}H_{36}BrCrN_2O_2S_2$: C, 28.78; H, 6.20; N, 4.79%.

***trans*-$[Cr(N_3)_2(dmpe)_2]BF_4$ (8).** The reaction of **1** (157 mg, 0.28 mmol) and NaN_3 (90 mg, 1.39 mmol) in aqueous methanol (50%, 30 cm^3) in the presence of zinc (300 mg) for 6 h gave a red solution. The filtered solution was diluted with water (500 cm^3) and applied on a column (ϕ 1.5 × 100 cm) of SP-Sephadex C-25 (Na^+ form). The adsorbed products were eluted with 0.05 mol dm^{-3} aqueous $NaBF_4$ solution, yielding a major red and a minor yellow-green band. The red eluate was concentrated to a volume of one-third under reduced pressure, and stored in a desiccator to give red crystals. Yield: 14 mg (10%). Found: C, 27.77; H, 6.21; N, 16.00%. Calcd for $C_{12}H_{32}BCrF_4N_6$: C, 27.55; H, 6.17; N, 16.07%.

***trans*-[CrCl(CN)(dmpe)$_2$]PF$_6$ (9).** A methanol solution (20 cm^3) containing **1** (380 mg, 0.67 mmol) and NaCN (72 mg, 1.47 mmol) was stirred for 30 min in the presence of zinc (300 mg), and then filtered. The filtrate was concentrated gradually in a desiccator to deposit orange crystals of **9**. The crude product was recrystallized from water. Yield: 158 mg (42%). Found: C, 27.77; H, 5.83; N, 2.91%. Calcd for $C_{13}H_{32}ClCrF_6NP_5$: C, 27.95; H, 5.77; N, 2.51%.

***trans*-[CrBr(CN)(dmpe)$_2$]ClO$_4$ (10).** A suspension of **3** (177 mg, 0.29 mmol) and NaCN (14 mg, 0.29 mmol) in aqueous acetone (50%, 50 cm^3) was stirred at 35 °C for 40 h, and then filtered. The filtrate was concentrated to ca. 5 cm^3 under reduced pressure, and applied on a column of Toyopearl HW-40 fine resin (ϕ 1 × 5 cm). The adsorbed products were eluted with water, giving a minor orange band, a major yellow-orange band, and a minor green band in this order. After elution of the orange band, aqueous methanol (50%) was used as an eluent. The yellow-orange eluate was concentrated to one-third of its volumn under reduced pressure, and further to dryness in a desiccator. The resulting crude product was recrystallized from aqueous (50%) methanol to give orange crystals of **10**. Yield: 54 mg (34%). Found: C, 27.89; H, 5.89; N, 2.41%. Calcd for $C_{13}H_{32}BrClCrNO_4P_4$: C, 28.00; H, 5.78; N, 2.51%.

***trans*-[Cr(CN)$_2$(dmpe)$_2$]PF$_6$ (11).** To an orange solution of **9** (150 mg, 0.27 mmol) in aqueous methanol (50%, 40 cm^3) were added KCN (200 mg, 3.07 mmol) and zinc (1.00 g) with stirring. The color of the mixture turned immediately into yellow. The mixture was filtered, and the filtrate was concentrated to 10 cm^3 under reduced pressure and stored in a desiccator to give yellow crystals of **11**. The product was recrystallized from water. Yield: 36 mg (25%). Found: C, 30.61; H, 5.82; N, 5.41%. Calcd for $C_{14}H_{32}Cr\ F_6N_2P_5$: C, 30.61; H, 5.87; N, 5.10%.

[CrBr$_3$(tdmme)] (13). A dichloromethane solution (10 cm^3) of [Cr(CO)$_3$(tdmme)] (190 mg, 0.49 mmol) was cooled in a dry ice-methanol bath. To the solution was added a dichloromethane solution (5 cm^3) of bromine (0.12 g, 0.75 mmol) dropwise with stirring. The mixture was stirred for 1 h at −78 °C, and the resulting orange precipitate was filtered off and dried in a vacuum desiccator for 1 h. During drying, the color of the product turned into bluish purple. The crude product was recrystallized from dichloromethane to give a dark blue powder, which was collected by filtration, washed with diethyl ether, and dried in vacuo. Yield: 0.21 g (79%). Found: C, 24.39; H, 4.97%. Calcd for $C_{11}H_{27}Br_3CrP_3$: C, 24.29; H, 5.00%.

[CrCl$_2$(CN)(tdmme)]·H$_2$O (14·H$_2$O) and [CrCl(CN)$_2$(tdmme)]·H$_2$O (15·H$_2$O). To a suspension of **12** (0.51 mmol) in methanol (30 cm^3) was added one or two equivalent amounts of NaCN. The mixture was refluxed for 20 h, and the resulting red solution was evaporated to dryness under reduced pressure. The residue was extracted with dichloromethane, and the extract was evaporated under reduced pressure to give a red-purple or red-orange powder. The crude product was recrystallized from methanol/diethyl ether. **14**·H$_2$O: red columnar crystals (51.4%). Found: C, 34.32; H, 7.09; N, 3.40%. Calcd for $C_{12}H_{29}C_{l2}CrNOP_3$: C, 34.38; H, 6.97; N, 3.34%. **15**·H$_2$O: orange needles (50.3%). Found: C, 38.04; H, 7.42; N, 7.39%. Calcd for $C_{13}H_{29}ClCrN_2OP_3$: C, 38.11; H, 7.13; N, 6.84%.

[Cr(CN)$_3$(tdmme)]·2H$_2$O (16·2H$_2$O). Complex **16**·2H$_2$O was prepared by a method similar to the above with three equivalent amounts of NaCN. Zinc (100 mg) was also added to the reaction mixture to give a better yield of the desired complex. Recrystallization from methanol/diethyl ether gave orange columnar crystals. Yield: 17%. Found: C, 39.93; H, 7.40; N, 9.75%. Calcd for $C_{14}H_{31}CrN_3O_2P_3$: C, 40.20; H, 7.47; N, 10.04%.

[Cr(NCS)$_3$(tdmme)] (17). A methanol solution (30 cm^3) containing **12** (53 mg, 0.13 mmol) and LiNCS (107 mg, 1.29 mmol) was refluxed for 24 h and then allowed to cool to room temperature. The reddish pink leaflet crystals which deposited were collected by filtration and dried in vacuo. Yield: 35 mg (58%). Found: C, 35.03; H, 5.76; N, 8.39%. Calcd for $C_{14}H_{27}CrN_3P_3S_3$: C, 35.14; H, 5.69; N, 8.78%.

[CrCl$_2$(tdmme)(PMe$_3$)]BPh$_4$·2H$_2$O (18). To a suspension of **12** (205 mg, 0.499 mmol) in methanol was added a toluene solution of trimethylphosphine (1 M, 0.50 cm^3, 0.50 mmol). The mixture was refluxed for 1 h, giving a reddish purple solution. After cooling to room temperature, the solution was filtered off, and the filtrate was concentrated to 10 cm^3 under reduced pressure. An excess amount of NaBPh$_4$ in methanol was added to the concentrate, inducing precipitation of a red-purple product. The crude product was collected by filtration and recrystallized from a mixture of acetonitrile and diethyl ether to deposit red-purple columnar crystals. Yield: 366 mg (95%). Found: C, 56.82; H, 7.11%. Calcd for $C_{38}H_{60}BCl_2CrP_4$: C, 56.59; H, 7.50%.

(NBu$_4$)[Cr(NCS)$_4$(dmpp)]. A mixture of anhydrous K$_3$[Cr(NCS)$_6$] (480 mg, 0.92 mmol) and dmpp (187 mg, 1.14 mmol) in ethanol (10 cm^3) was refluxed for 10 min, and then filtered. To the filtrate was added [NBu$_4$]ClO$_4$ (317 mg, 0.93 mmol), yielding a red precipitate. The crude product collected by filtration was recrystallized from acetone. Yield: 300 mg (47%). Found: C, 46.41; H, 7.84; N, 10.19%. Calcd for $C_{27}H_{54}CrN_5P_2S_4$: C, 46.94; H, 7.84; N, 10.19%.

X-ray Crystallographic Study. The X-ray diffraction data collection and structural calculation were performed by our standard technique as described previously,[27] using a Rigaku automated four-circle diffractometer AFC-7R equipped with graphite monochromated Mo-$K\alpha$ radiation (λ = 0.71073 Å) and a TeXsan software package[28] (the structures were solved by SHELXS-86 program[29]), respectively. For complex **6**, a Laue symmetry check and systematic absences indicated that the space group was either *Cm*, *C*2 or *C*2/*m*. The centrosymmetric *C*2/*m* was chosen, and the structure was successfully solved and refined under this assumption. Complex **16**·2H$_2$O was found to be isomorphic to the corresponding cobalt(III) complex, [Co(CN)$_3$(tdmme)]·2H$_2$O,[22] and, therefore, the non-centrosymmetric space group, *Pna*2$_1$, was chosen. The structure model based on this space group could not be transferred to that of the corresponding centrosymmetric *Pnam*.

Crystal data are: **6**, $C_{14}H_{36}CrI_3P_4$, 0.4 × 0.2 × 0.1 mm, monoclinic, *C*2/*m*, a = 13.1053(7), b = 10.373(1), c = 10.3997(7) Å, β = 115.442(4)°, U = 1276.6(2) Å^3, Z = 2, D_c = 1.980 Mg m^{-3}, μ = 4.324 mm^{-1}, A (transmission factor) = 0.839–1.000, $R(F)$ = 0.022 for 1717 independent reflections with $I > 3\sigma(I)$. **16**·2H$_2$O, $C_{14}H_{31}CrN_3O_2P_3$, 0.4 × 0.2 × 0.15 mm, orthorhombic, *Pna*2$_1$, a = 17.799(2), b = 9.484(1), c = 13.153(1) Å, U = 2220.3(4) Å^3, Z = 4, D_c = 1.251 Mg m^{-3}, μ = 0.741 mm^{-1}, A = 0.729–0.917, $R(F)$ = 0.054 for 1588 independent reflections with $I > 3\sigma(I)$.

Tables of crystallographic data (excluding structure factors), atomic coordinates, thermal parameters, and full list of bond lengths and angles are deposited as Document No. 74036 at the Office of the Editor of Bull. Chem. Soc. Jpn. Crystallographic data have been deposited at the CCDC, 12 Union Road, Cambridge CB2 1EZ, UK and copies can be obtained on request, free of charge, by quoting the publication citation and deposition numbers CCDC 138493 and 138494.

Results and Discussion

Syntheses and Structural Assignment of Complexes. *trans*-[CrX$_2$(dmpe or dmpp)$_2$]$^+$ (X = Cl, Br, or I). Although complexes of *trans*-[Cr(Cl or I)$_2$(dmpe)$_2$]$^+$ were already synthesized by Salt et al., they employed rather complicated preparative procedures; for example, the dichloro complex was obtained by oxidation of *trans*-[Cr^{II}Cl$_2$(dmpe)$_2$] or reduction of [Cr^{IV}H$_2$Cl$_2$(dmpe)$_2$].[6] Thus in this study we attempted to prepare the complex by the following simple method starting from CrCl$_3$·6H$_2$O. A reaction of [CrCl$_3$(DMF)$_3$] (DMF = *N*,*N*-dimethylformamide), which was in situ prepared from CrCl$_3$·6H$_2$O by heating its DMF solution,[30] with dmpe in DMF, followed by addition of NaPF$_6$, gave green crystals of *trans*-[CrCl$_2$(dmpe)$_2$]PF$_6$ (**1**) in 58% yield. Even though an excess amount of dmpe was employed in the reaction, formation of the tris(dmpe) complex, [Cr(dmpe)$_3$]$^{3+}$, could not be detected; complex **1** was the only isolable product from the reaction mixture. The analogous dmpp complex, *trans*-[CrCl$_2$(dmpp)$_2$]PF$_6$ (**2**), could not be prepared by a method similar to that for the above dmpe complex **1**, but it was obtained by a direct reaction between anhydrous CrCl$_3$ and dmpp at 140 °C, followed by treatment with 2-methoxyethanol and crystallization with NaPF$_6$, though the yield was low (10%). For preparation of the corresponding dibromo complexes, *trans*-[CrBr$_2$(dmpe)$_2$]ClO$_4$ (**3**) and *trans*-[CrBr$_2$(dmpp)$_2$]PF$_6$ (**4**), it was necessary to use [CrBr$_2$(en)(OH$_2$)$_2$]Br instead of (hydrated or anhydrous) chromium(III) bromide as a starting chromium(III) source. The diiodo complexes, *trans*-[CrI$_2$(dmpe)$_2$]I (**5**) and *trans*-[CrI$_2$(dmpp)$_2$]I (**6**), were obtained in high yields (80–85%) from CrI$_3$·6H$_2$O in propanol.

The *trans* geometries of the complexes, **1**–**6**, are suggested by UV-vis spectroscopy, in addition to the X-ray structural analysis of **6** (*vide infra*). The absorption spectra of complexes **1**–**6** (Fig. 1) are similar in pattern to one another, and also similar to those of *trans*-[Cr(Cl or Br)$_2$(diphos or diars)$_2$]$^+$,[2,3] although the diiodo complexes **5** and **6** show additional absorption bands around 24000–30000 cm^{-1}. Further, the spectral patterns of complexes **1**–**6** are rather similar to those of *trans*-[CoX$_2$(dmpe or dmpp)$_2$]$^+$, whose geometrical structures have been determined by NMR spectroscopy, but very different from those of the *cis*-isomers.[18]

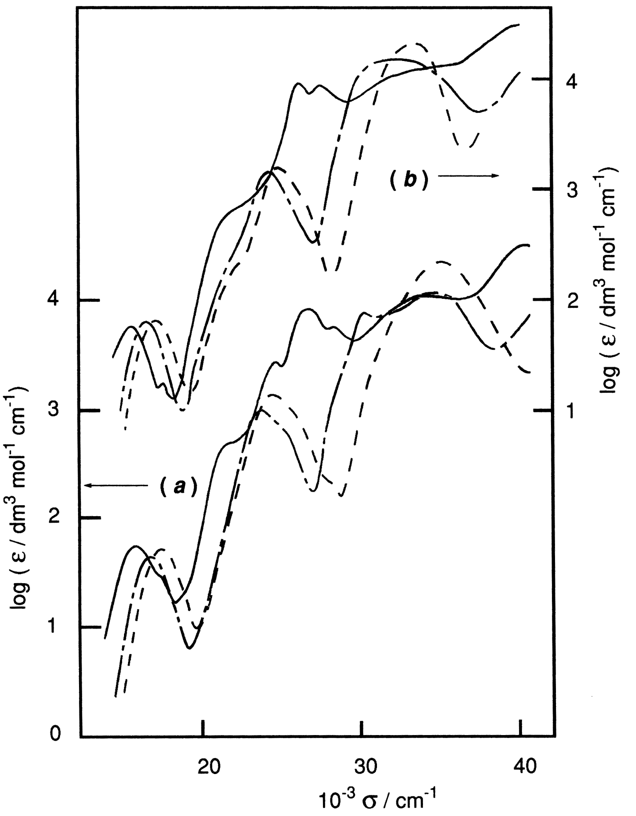

Fig. 1. Absorption spectra of (*a*) *trans*-[CrX$_2$(dmpe)$_2$]$^+$ and (*b*) *trans*-[CrX$_2$(dmpp)$_2$]$^+$ (X = Cl (----) in acetonitrile, Br (– – –) in acetonitrile and I (—) in methanol) at room temperature.

Pseudohalogeno–Bis(dmpe) Complexes. Complexes of *trans*-[Cr(NCS)$_2$(dmpe)$_2$]$^+$ and *trans*-[Cr(N$_3$)$_2$(dmpe)$_2$]$^+$ were prepared by reactions of **1** with NH$_4$NCS and with NaN$_3$, and isolated as orange crystals of the Br$^-$ salt (**7**) and red ones of the BF$_4$$^-$ salt (**8**), respectively. The infrared spectrum of complex **7** showed a sharp strong ν(C–N) band at 2055 cm^{-1} and a broad weak band due to the ν(C–S) around 800 cm^{-1}, indicating two mutually *trans* N-bonded thiocyanate ligands.[31,32]

In contrast to the above results, a similar reaction of **1** with NaCN in methanol yielded only orange-red crystals of *trans*-[CrCl(CN)(dmpe)$_2$]PF$_6$ (**9**), even though an excess amount of NaCN was applied. The dicyano complex, *trans*-[Cr(CN)$_2$(dmpe)$_2$]PF$_6$ (**11**), was obtained as yellow crystals by a reaction of complex **9** and KCN in aqueous methanol. In the case of a reaction of **3** with an equimolar amount of NaCN in aqueous acetone, the reaction mixture contained three complexes. They were separated by column chromatography into **3** (green), *trans*-[CrBr(CN)(dmpe)$_2$]ClO$_4$ (**10**; orange) and *trans*-[Cr(CN)$_2$(dmpe)$_2$]ClO$_4$ (yellow). The infrared spectra of complexes **9**–**11** were similar to those of complexes **1** and **3** except for ν(C–N) bands, indicating the *trans* configuration of the complexes.[31,33] The weak ν(C–N) stretching band was observed around 2110–2115 cm^{-1}, as observed for the corresponding en complexes.[33] No corresponding *cis*-isomers were found for [CrX$_2$(dmpe or dmpp)$_2$]$^+$-type complexes.

Tripodal Tridentate Phosphine (tdmme) Complexes. The complex [CrCl$_3$(tdmme)] (**12**) was prepared in a relatively high yield from anhydrous CrCl$_3$ and tdmme in tetrahydrofuran,[11] but the corresponding tribromo complex, [CrBr$_3$(tdmme)] (**13**), could not be obtained by a similar method using chromium(III) bromide or [CrBr$_2$(en)(H$_2$O)$_2$]Br. Then we attempted to prepare the complex **13** by oxidation of tricarbonylchromium(O) with bromine. A reaction of [Cr(CO)$_3$(tdmme)][27] and Br$_2$ in dichloromethane at −78 °C afforded an orange precipitate, which was unstable at room temperature even in the solid state and converted to bluish purple powder under reduced pressure. Recrystallization of the resulting powder from dichloromethane yielded dark blue microcrystals of complex **13**.

As with the bis(dmpe) complexes, a successive substitution reaction of complex **12** with NaCN in methanol gave red co-

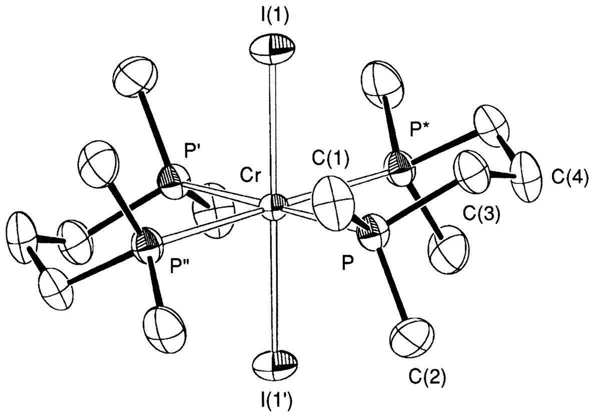

Fig. 2. Perspective drawing (50% probability level) of the cationic part of *trans*-[CrI$_2$(dmpe)$_2$]I. Hydrogen atoms are omitted for clarity.

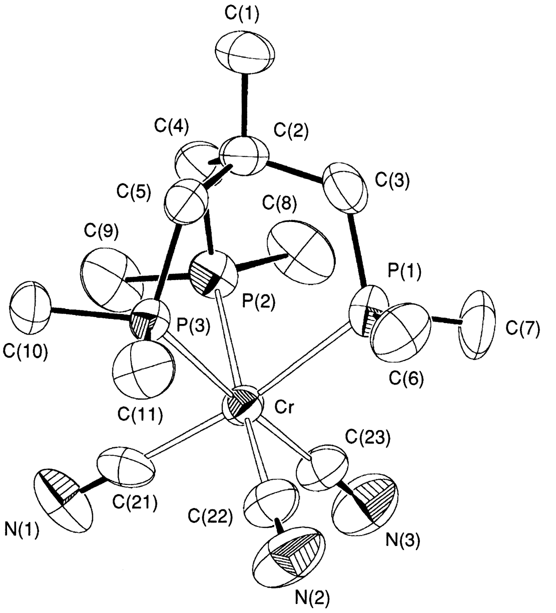

Fig. 3. Perspective drawing (50% probability level) of [Cr(CN)$_3$(tdmme)]. Hydrogen atoms are omitted for clarity.

lumnar crystals of [CrCl$_2$(CN)(tdmme)]·H$_2$O (**14**·H$_2$O), orange needles of [CrCl(CN)$_2$(tdmme)]·H$_2$O (**15**·H$_2$O) and yellow needles of [Cr(CN)$_3$(tdmme)]·2H$_2$O (**16**·2H$_2$O). Also, a tris(thiocyanato-*κN*) complex of [Cr(NCS)$_3$(tdmme)] (**17**) was prepared from complex **12** and LiNCS.

The substitution by PMe$_3$ for one of the Cl$^-$ ligands in [CrCl$_3$(tdmme)] was attempted to prepare [CrCl$_2$(tdmme)-(PMe$_3$)]$^+$, since the complex has a set of donor atoms of *cis*-[CrCl$_2$P$_4$], which is considered as a counterpart of complexes **1** and **2** (*trans*-[CrCl$_2$P$_4$]) in a pair of geometrical isomers, as far as their chromophores are concerned. Addition of a toluene solution of PMe$_3$ to a suspension of **12** in methanol afforded a red-purple solution, from which the desired complex could be isolated as the BPh$_4^-$ salt (**18**).

Crystal Structures. ***trans*-[CrI$_2$(dmpp)$_2$]I (6).** The X-ray analysis revealed that complex **6** crystallized in a monoclinic space group *C*2/*m* with *Z* = 2. The Cr and I(2), the counter anion, atoms are located at the positions having the site symmetry of 2/*m*, while the I(1) and C(4) are on the crystallographic plane of symmetry. A perspective view of *trans*-[CrI$_2$(dmpp)$_2$]$^+$ is shown in Fig. 2. The six-membered chelate ring of dmpp takes a typical chair conformation. The bite angle of dmpp is 87.79(3)°, which is larger and closer to the right angle than that of dmpe forming a five-membered chelate ring in *trans*-[CrCl$_2$(dmpe)$_2$]BPh$_4$ (83.0(2)°).[6] The Cr–P bond length in the dmpp complex **6**, 2.5147(6) Å, is longer by 0.07 Å than those in the above-mentioned dmpe complex (2.442(5) and 2.447(5) Å). Such longer metal(III)–P bonds of dmpp than those of dmpe are also found in the analogous cobalt(III)[34] and rhodium(III)[24] complexes, but the difference is pronounced in the present chromium(III) complexes. The CrI(1) bond length is 2.6619(3) Å.

[Cr(CN)$_3$(tdmme)] (16). The molecular structure of complex **16** is depicted in Fig. 3, and selected structural parameters are collected in Table 1. The Cr–P bond lengths (av 2.455 Å) are similar to those in [CrCl$_3$(tdmme)] (**12**: av 2.458 Å).[11] This fact contrasts with the case of the analogous cobalt(III) complexes; the Co–P bonds in [Co(CN)$_3$(tdmme)] (av 2.228 Å) are slightly longer than those in [CoCl$_3$(tdmme)] (av 2.203 Å), indicating the *trans* influence of CN$^-$ is stronger than that of Cl$^-$.[22] The average Cr–C bond lengths in **16** (2.05 Å) are a little shorter than those in Cs$_2$K[Cr(CN)$_6$] (2.072 Å at ambient

Table 1. Selected Bond Lengths (Å), Bond Angles (°), Torsion Angles (°) and Hydrogen-Bond Distances (Å) for Complex **16**·2H$_2$O

Cr–P(1)	2.451(3)	Cr–P(2)	2.455(3)	Cr–P(3)	2.459(3)
Cr–C(21)	2.07(1)	Cr–C(22)	2.03(1)	Cr–C(23)	2.05(1)
C(21)–N(1)	1.13(1)	C(22)–N(2)	1.14(1)	C(23)–N(3)	1.12(1)
P(1)–Cr–P(2)	84.05(9)	P(1)–Cr–P(3)	84.26(9)	P(2)–Cr–P(3)	84.79(10)
P(1)–Cr–C(21)	171.6(3)	P(2)–Cr–C(22)	174.2(3)	P(3)–Cr–C(23)	176.3(3)
Cr–C(21)–N(1)	177(1)	Cr–C(22)–N(2)	179(1)	Cr–C(23)–N(3)	177(1)
Cr–P(1)–C(3)–C(2)	22.0(9)	Cr–P(2)–C(4)–C(2)	23.0(9)		
Cr–P(3)–C(5)–C(2)	22.2(8)				
O(1)···N(1)	2.93(1)	O(2)···N(2)	2.84(1)		
O(2)···N(3)	2.88(1)	O(1)···O(2)	2.65(2)		

Table 2. Absorption (AB)[a),b)] and Magnetic Circular Dichroism (MCD)[a),c)] Spectral Data of Complexes

Complex	Method	d–d bands		CT bands	
1	AB	17.40(50), 26.05^{sh}(ca. 560)	24.36(1380),	31.9^{sh}(ca. 7500), 44.0^{sh}(10000)	34.95(20400),
	MCD	19.08(−0.002), 26.1(−0.31)	24.42(+0.95),	31.83(+2.63),	36.2(−0.53)
2	AB	17.05(66), 24.8(1550)	22.0^{sh}(ca.190),	33.7 (21900),	43.8^{sh}(ca. 12000)
	MCD	19.0(−0.0045), 26.55(−0.25)	24.75(+0.61),	31.5(+1.80),	34.9(−0.64)
3	AB	16.74(44), 27.5^{sh}(ca. 500)	23.7(1000),	30.2(7580), 45.45(26900)	34.6(9780),
	MCD	18.73(−0.0063), 25.4(−0.78)	23.67(+0.81),	30.3(+3.60), 36.3(+4.90)	32.4(−3.68),
4	AB	16.30(65), 24.2(1350)	21.6^{sh}(ca. 190),	30.6^{sh}(14000),	33.2(15500)
	MCD	23.92(+0.85),	26.4(−0.83)	29.8(+1.67), 35.2(+3.4)	32.7(−2.92),
5	AB	15.76(51), 21.3^{sh}(485),	17.7^{sh}(26), 24.5(2690)	26.7(8130), 33.9(10700),	28.25(5620), 39.8(30900)
6	AB	15.40(60), 21.3^{sh}(570)	17.60(24),	26.1(7940), 33.9^{sh}(ca. 11000)	27.69(7769), 40.0(26900)
7	AB	20.0^{sh}(ca. 120),	23.0(890)	26.50(24000),	34.0(14000)
8	AB	18.3(176),	22.5(790)	27.4(6300),	32.0(17800)
9	AB	21.65(437),	25.36(1260)	30.29(3470),	38.04(21400)
	MCD	26.2(+0.63),	27.3(−0.21)	30.3(+2.60), 37.5(−0.70)	36.2(+0.74),
10	AB	21.3(174),	24.7(1170)	29.3(4570)	37.2(19500)
11	AB	25.05^{sh}(1960)		28.49(3720),	39.21(22400)
	MCD	25.0(+0.31)		28.6(+2.46), 40.8(−1.82)	37.1(+1.09),
12	AB	17.05(676),	21.3(204)	31.75(5620),	36.0(12300)
	MCD	17.0(−0.045), 21.4(+0.017)	18.0,	30.35(−0.57),	32.0(+5.1)
13	AB	16.6(794),	20.65(389)	30.55(7410),	34.3(ca. 7940)
	MCD	16.6(−0.47), 20.7(+0.14)	17.6,	28.9(+3.6), 31.85(+0.36), 35.65(+0.72)	31.0(±0), 33.6(−1.9),
14	AB	19.9(200)		30.1(4100)	
15	AB	20.8(134)		27.5^{sh}(ca. 800),	29.2(3440)
16	AB	24.6^{sh}(ca. 320)		29.1(3980),	34.9(1410)
17	AB	20.05(490)		27.1(11000), 35.2(5000)	29.8(7940),
18	AB	18.0(398),	24.1(148)	28.7^{sh}(ca. 890), 36.4(11220),	31.2(3300), 37.5(12300)

a) ^{sh} denotes shoulder feature. b) $10^{-3}\ \sigma/\mathrm{cm}^{-1}$ ($\varepsilon/\mathrm{dm}^3\ \mathrm{mol}^{-1}\ \mathrm{cm}^{-1}$).
c) $10^{-3}\ \sigma/\mathrm{cm}^{-1}$ ($\Delta\varepsilon_\mathrm{M}/\mathrm{dm}^3\ \mathrm{mol}^{-1}\ \mathrm{cm}^{-1}\ \mathrm{T}^{-1}$).

temperature; 2.066 Å at 120 K),[35] but the experimental errors are too large to discuss such a small difference of 0.02 Å. Therefore, it is concluded that neither CN^- nor tdmme exert apparent *trans* influence in the chromium(III) complex.

The spectroscopic Properties of the Complexes. The UV-vis absorption and MCD spectral data of the complexes prepared in this study are collected in Table 2.

Ligand-Field Parameters of [CrX$_3$(tdmme)] (X = Cl, Br, CN and NCS). In the visible absorption spectra of the trichloro (**12**) and tribromo (**13**) complexes (Fig. 4), two characteristic bands are observed at 17050 and 21300 cm^{-1} for **12** and at 16600 and 20650 cm^{-1} for **13**. These absorption bands can be assigned to the first ($^4A_2 \rightarrow {}^4T_2$) and the second ($^4A_2 \rightarrow {}^4T_1$) spin-allowed d–d transitions in holohedrized O_h symmetry. The tris(thiocyanato-κN) complex **17** gives the $^4A_2 \rightarrow {}^4T_2$ band at 20050 cm^{-1}, and the tricyano complex **16** shows such a transition as a shoulder around 24600 cm^{-1}. The $^4A_2 \rightarrow {}^4T_1$ transition band of complexes **16** and **17** are obscured by the low-lying charge-transfer bands.

The observed $^4T_2$ and $^4T_1$ transition energies of complexes **12** and **13** give ligand-field and Racah's interelectronic repulsion parameters[14,36,37] as follows: Δ(d) = 17050 and B = 354

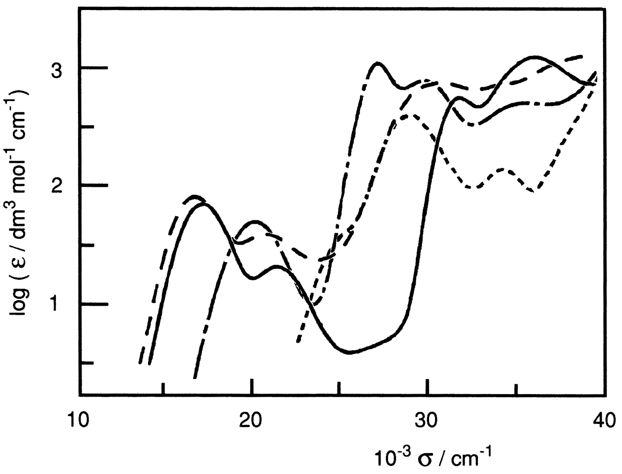

Fig. 4. Absorption spectra of $[CrX_3(tdmme)]$ in CH_2Cl_2 at room temperature (X = Cl (—), Br (----), CN (······) and NCS (‒ ‒ ‒)).

cm^{-1} for complex **12**; Δ(d) = 16600 and B = 338 cm^{-1} for complex **13**.[38] When the rule of average environment for a mixed ligand complex is applied, the values[37] of Δ_{Cl} = 13180 and Δ_{Br} = 12340 cm^{-1} lead to the parameter of Δ_{tdmme} = 20920 (for **12**) and 20860 (for **13**) cm^{-1}. Compared to the parameters of Δ_{tacn} = 20240 and B = 454 cm^{-1} for $[CrBr_3(tacn)]$ (tacn = 1,4,7-triazacyclononane),[39] it can be stated that the ligand-field perturbation on chromium(III) by tdmme is almost the same as that by tacn, while the nephelauxetic effect of tdmme is remarkably larger.

The MCD spectra of complexes **12** and **13** show a weak negative and a weak positive component, corresponding to the $^4T_2$ and $^4T_1$ transitions, respectively, in addition to a sharp dispersion-type component observed at 18000 for **12** and 17600 cm^{-1} for **13**. These sharp components are presumably assigned to the spin-forbidden d–d ($^4A_2 \rightarrow {}^2T_2$) transition. Other spin-forbidden d–d transitions ($^4A_2 \rightarrow {}^2T_1$, ^2E), which are expected to be lower in energy than the $^2T_2$ transition, are not observed. From such a spin-forbidden transition energy, the parameter B can be estimated,[38] if $C = 4B$ is assumed, as 514 and 503 cm^{-1} for complexes **12** and **13**, respectively. These values of B are far larger than those estimated by the $^4T_1$ transition energies. To explain the inconsistency of these B values, one should note that the interelectronic repulsion between the t_{2g} and e_g subshells is reduced in a large extent from that within the t_{2g} subshell.[3] In the other word, the B_{35} value is much smaller than the corresponding B_{55} one, which would be indicative of a strong σ-covalency of the Cr^{III}–P bond in the tdmme complexes.

Ligand-Field Parameters of *trans*-$[Cr(Cl\ or\ Br)_2(dmpe\ or\ dmpp)_2]^+$. Complexes **1–6** with holohedrized D_{4h} symmetry are expected to give four spin-allowed d–d ($^4B_1 \rightarrow a^4E$, $^4B_2$, $^4A_2$ and b^4E) transition bands, similar to the analogous en complexes, *trans*-$[CrX_2(en)_2]^+$.[40,41] The absorption spectra of complexes **1–4** show a medium intensity (ε = 49–66 $dm^3\ mol^{-1}\ cm^{-1}$) band in the region of 15400–17300 cm^{-1}, which can be assigned as the $^4B_1 \rightarrow a^4E$ transition band. Around 20000–30000 cm^{-1} an absorption envelope is observed. The corresponding absorption envelope of *trans*-$[CrX_2(en)_2]^+$ is assigned as the overlapped components due to the $^4B_1 \rightarrow {}^4B_2$, $^4A_2$ and b^4E transitions.[40,41] However, the band intensities of the dmpe and dmpp complexes, **1–4**, are remarkably larger (ε = 1000–1500 $dm^3\ mol^{-1}\ cm^{-1}$) than those of the en complexes ($\varepsilon \leq 40$ $dm^3\ mol^{-1}\ cm^{-1}$). For the analogous diphos[2] and diars[3] complexes, the corresponding absorption envelope with similarly large intensity has been observed in a similar region, and assigned as the overlapped $^4B_2$, b^4E and $^4A_2$ transition bands without any comment about their high intensities or the different order of the $^4A_2$ and b^4E transition bands. To examine these strong bands in more detail, the Gaussian curve analysis of the absorption spectra and the measurement of MCD spectra have been performed.

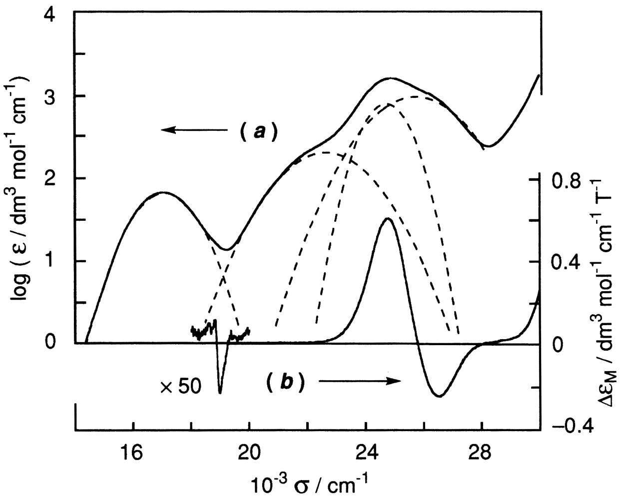

Fig. 5. (*a*) The absorption spectrum with the components from the Gaussian curve analysis and (*b*) the MCD spectrum of *trans*-$[CrCl_2(dmpp)_2]PF_6$ (**2**, CH_3CN, r.t.) in the visible region.

For the dichlorobis(dmpp) complex **2**, the spectral shape of the absorption envelope in the region of 20000–30000 cm^{-1} indicates clearly that there are three components. The Gaussian curve analysis of the absorption envelope resolved the spectrum into three bands centered at 22640 (ε = 201), 24720 (ε = 806) and 25750 cm^{-1} (ε = 987 $dm^3\ mol^{-1}\ cm^{-1}$), as shown in Fig. 5. The MCD spectrum of **2** in this region shows a positive and a negative peak. The positive peak is located at 24750 cm^{-1}, which coincides well with the energy of the second component in the above Gaussian analysis. On the other hand, the negative peak is located at 26550 cm^{-1}, which is higher in energy (by 800 cm^{-1}) than the position of the highest-energy Gaussian component. However, if we assume that this transition component gives a negative MCD A term, then the position at $\Delta\varepsilon_M = 0$ (25790 cm^{-1}) coincides with that of the highest-energy Gaussian component. The MCD peak corresponding to the lowest-energy Gaussian component, as well as that to the $^4B_1 \rightarrow a^4E$ transition band, are much weaker than the above two. These features of the MCD spectrum allow us to assign the three Gaussian components in the overlapped absorption envelope as the $^4B_1 \rightarrow {}^4B_2$, $^4A_2$ and b^4E transition bands.

On the basis of the above-mentioned assignments for the transition bands and their energies for complex **2**, the ligand-field[36] and B (B_{35}) parameters of complex **2** are calculated as follows:[38] Δ(d) = 18940, Δ(e) = 4390, Δ(t_2) = 2260, and B_{35} = 539 cm^{-1}. The rule of average environment and the value of Δ_{Cl} = 13180 cm^{-1} lead to the parameter of Δ_{dmpp} = 21830 cm^{-1}. It is notable that the ligand-field perturbation energy of dmpp, Δ_{dmpp}, is slightly larger than that of tdmme, Δ_{tdmme}, although the Cr–P bonds in the dmpp complex **6** is longer than those in the tdmme complex **16**.

The MCD spectrum of complex **2** shows a sharp negative component at 19000 cm^{-1} (Fig. 5), which would be assigned as the spin-forbidden d–d ($^4B_1 \rightarrow {}^4E$, $^4B_2$) transition. Such a transition energy gives the parameter B_{55}, similarly to complexes **12** and **13**, and the value is estimated as 543 cm^{-1}. Differing from complexes **12** and **13**, the values of B_{35} and B_{55} are almost equal to each other for complex **2**.

The dibromobis(dmpp) complex, **4**, is treated in a similar manner. The energy of $E_{obs}(a^4E)$ = 16300 cm^{-1} and three Gaussian components, $E_{obs}(^4B_2)$ = 22250, $E_{obs}(^4A_2)$ = 23930 and $E_{obs}(b^4E)$ = 25750 cm^{-1}, lead to the set of parameters: Δ(d) = 18370, Δ(e) = 5350, Δ(t_2) = 2190, and B_{35} = 564 cm^{-1}. The resulting Δ(d) value and Δ_{Br} = 12340 cm^{-1} give Δ_{dmpp} = 21350 cm^{-1} for complex **4**. It is interesting to compare, here, the spectroscopic properties of the dmpp complexes with those of the corresponding en complexes.[42] All three ligand-field parameters of Δ(d), Δ(e) and Δ(t_2), as well as the interelectronic replusion parameter B_{35}, of the dmpp complexes are very similar to those of the en complexes. However, the band intensities, especially those of the $^4A_2$ and b^4E transitions, of the dmpp complexes are much larger. As described in the following subsection, the phosphine complexes show intense charge-transfer transition bands which are close in energy to the d–d bands. The intensity-stealing mechanism (or partial mixing of the d–d excited state with the CT one) would make the band intensities larger.

The dmpe complexes of **1** and **3**, in contrast to the dmpp complexes above, do not show a clear shoulder feature at the lower energy side of the absorption envelope around 20000–30000 cm^{-1}. The Gaussian curve analysis to resolve the absorption envelope gives only two components centered at 24480 and 25540 cm^{-1} for **1** and 23480 and 24420 cm^{-1} for **3**. These Gaussian components are probably assigned as the $^4B_1 \rightarrow {}^4A_2$ and b^4E transition bands, because their MCD spectra are similar to complex **2**. Although the $^4B_1 \rightarrow {}^4B_2$ transition energy can not be obtained experimentally, the spin-forbidden d–d ($^4B_1 \rightarrow {}^4E$, $^4B_2$) band is observed in their MCD spectra at 19080 and 18730 cm^{-1} for complexes **1** and **3**, respectively. These transition energies lead to the B_{55} values of 545 and 535 cm^{-1} for **1** and **3**, respectively. Provided that the B_{35} value is the same as the B_{55} one, as in complex **2**, then the ligand-field parameters for the dmpe complexes **1** and **3** can be estimated. The results are: Δ(d) = 18140, Δ(e) = 1610 and Δ(t_2) = 960 cm^{-1} for complex **1**; Δ(d) = 17270, Δ(e) = 1260 and Δ(t_2) = 635 cm^{-1} for complex **3**. The ligand-field perturbation energy of dmpe, Δ_{dmpe}, is then calculated as 20620 and 19740 cm^{-1} for complexes **1** and **3**, respectively, which are a little smaller than Δ_{dmpp} and Δ_{en}. Further, it is remarkable that the Δ(e) and Δ(t_2) values of dmpe complexes are much reduced from those of the corresponding dmpp and en complexes.

The d–d Transition Bands of $[CrCl_2(tdmme)(PMe_3)]^+$. The complex, **18**, shows two d–d bands at 18000 (ε = 398) and 24000 cm^{-1} (ε = 148 $dm^3\ mol^{-1}\ cm^{-1}$), both of which are higher in energy than those of complex **12**. However, the explicit band splitting due to lowering the molecular symmetry from O_h is not observed, as also for *cis*-$[CrCl_2(en)_2]^+$.[40] At the most rough approximation (the averaged transition energies and O_h symmetry are assumed), the ligand-field and repulsion parameters are estimated as Δ(d) = 18000 and B_{35} = 500 cm^{-1}, and the ligand-field strength of PMe_3, Δ_{PMe_3}, in complex **18** is calculated as 18900 cm^{-1}. The B_{35} value of complex **18** is larger than that of complex **12**, and nearly equal to the value of complex **2**. We can not explain explicitly the reason for the difference in such B_{35} values at present, but it may be stated that the extremely small B_{35} value is so far limited for complexes of $[Cr(Cl\ or\ Br)_3(tdmme)]$ (**12** and **13**).

Spectra of the Pseudohalogeno Complexes. In the previous subsection, we have found that dmpp gives a similar ligand-field perturbation to en, while dmpe has a little smaller value, in *trans*-$[CrX_2(L–L)_2]^+$-type complexes. In contrast, the spectral patterns of dicyano complexes, **11** and *trans*-$[Cr(CN)_2(en)_2]^+$,[33] are very different from each other. This fact results from a low-lying charge-transfer band existing at almost the same energy as the d–d bands, which is clearly shown in the MCD spectra. Figure 6 compares the UV-vis and MCD spectra of a series of complexes, *trans*-$[Cr(Cl\ or\ CN)_2(dmpe)_2]PF_6$ (**1**, **9** and **11**). As one can expect from the large difference in the ligand-field strengths between Cl^- and CN^-,[14,15,43] the d–d transition bands are blue-shifted as the number of CN^- increases. The MCD component due to the $^4B_1 \rightarrow {}^4A_2$ transition is observed at 24400, 25300 and 25900 cm^{-1} for **1**, **9** and **11**, respectively, with decreasing the MCD intensity in this order. In contrast, the lowest-energy charge-transfer band is red-shifted in the reversed order: **1** (31800) > **9** (30300) > **11** (28600 cm^{-1}), which is observed as a sharp and strong positive component in their MCD spectra and as a band or a shoulder in their absorption spectra (Fig. 6). Thus, in the dicyano complex **11** the intense CT band obscures the weaker d–d transition bands, showing the spectral pattern of **11** different from that of *trans*-$[Cr(CN)_2(en)_2]^+$.

In addition to the above-mentioned lowest-energy CT band, the second CT transition is observed as a very intense band in the absorption spectra and gives a dispersion-type (negative A term) component in the MCD spectra. The second CT band is blue-shifted on increasing the number of CN^- ligands: **1** (34950) < **9** (38040) < **11** (39210 cm^{-1}), in contrast to the first CT band. The bromo-cyano series of complexes, **3**, **10** and **11**, gives the same tendency for the first (**3**: 30300 > **10**: 29300 > **11**: 28600 cm^{-1}) and the second (**3**: 34600 < **10**: 37200 < **11**: 39210 cm^{-1}) CT bands. When the CT energies of the chloro-cyano and bromo-cyano series of complexes are compared, it is obvious that the first CT energy decreases in the axial ligand order of $Cl^- > Br^- > CN^-$, while the second one increases in the order of $Br^- \leq Cl^- < CN^-$. Despite the different configuration of the donor atom sets, the tdmme complexes of **12–16** give a similar tendency for their two low-lying CT bands energies (see Table 2). These CT bands are presumably assigned as the P(σ)-to-Cr(dσ) and X(σ or π)-to-Cr(dσ) charge-transfer transitions, as suggested for the corresponding cobalt(III) com-

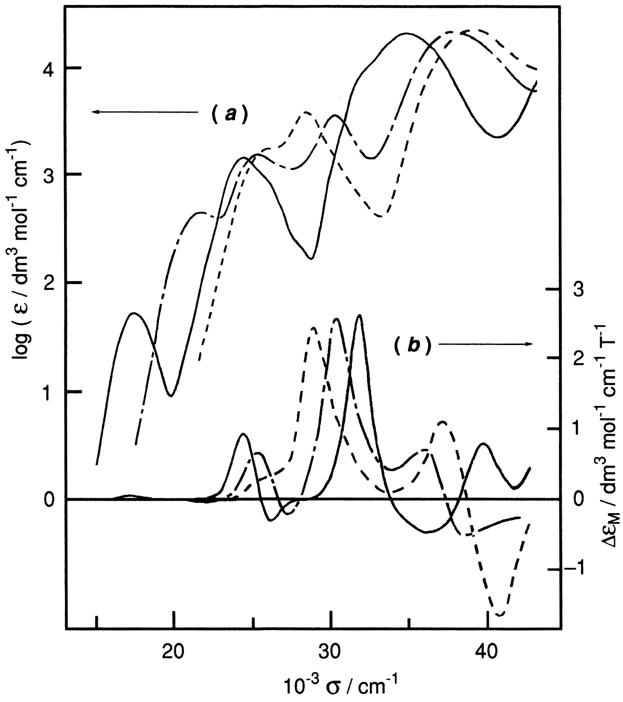

Fig. 6. (*a*) Absortion and (*b*) MCD spectra of *trans*-[$\mathrm{CrCl}_n(\mathrm{CN})_{2-n}(\mathrm{dmpe})_2$]$\mathrm{PF}_6$ (n = 2 (—), 1 (- - -) or 0 (----)) in acetonitrile at room temperature.

plexes.[18] However, we can not assign them definitely at present, since the P(σ)-to-Cr(dπ) and X(σ or π)-to-Cr(dπ) CT transitions are also possible for the present chromium(III) complexes.

The diazido complex **8** shows two absorption bands assignable to the d–d transitions at 18300 and 22500 cm^{-1}. In contrast, the d–d transitions of the bis(thiocyanato-κN) complex **7** are observed as shoulders around 20000 and 23000 cm^{-1}, together with a very intense sharp band at 26500 cm^{-1}. A similarly intense sharp band in this region has also been observed for other chromium(III) complexes containing both thiocyanate and phosphine ligands such as [$\mathrm{Cr(NCS)_3(tdmme)}$] (**17**), ($\mathrm{NBu_4}$)[$\mathrm{Cr(NCS)_4(dmpp)}$] ($\sigma$ = 27000 cm^{-1}, ε = 6460 $\mathrm{dm}^3\,\mathrm{mol}^{-1}\,\mathrm{cm}^{-1}$) and [$\mathrm{Cr(NCS)_4}$(monodentate phosphine)$_2$]$^-$.[44] However, neither the analogous thiocyanato–amine complexes such as *trans*-[$\mathrm{Cr(NCS)_2(en)_2}$]$^+$ [44] and [$\mathrm{Cr(NCS)_3(tacn)}$],[39] nor the halogeno–phosphine complexes as **1** and **12** show the corresponding absorption band. Thus, this characteristic band seems to arise in the phosphine-thiocyanate chromium(III) complexes, but the origin is still unknown.

Concluding Remarks

Three series of chromium(III)-phosphine complexes, *trans*-[$\mathrm{CrX_2(dmpe)_2}$]$^+$, *trans*-[$\mathrm{CrX_2(dmpp)_2}$]$^+$ and [$\mathrm{CrX_3(tdmme)}$], in addition to [$\mathrm{CrCl_2(dmpe)_2(PMe_3)}$]$^+$, have been prepared and their structures and spectroscopic properties have been investigated. The X-ray analyses of complexes **6** and **16**$\cdot$2$\mathrm{H_2O}$, together with that of *trans*-[$\mathrm{CrCl_2(dmpe)_2}$]$\mathrm{BPh_4}$,[6] have indicated, though the (pseudo)halogeno ligands are different from one complex to another, that the Cr–P bond lengths become longer in the order of dmpe < tdmme < dmpp. In contrast, the ligand-field strengths (in the Cl complexes) becomes larger in this order: Δ_{dmpe} (20620) < Δ_{tdmme} (20920) < Δ_{dmpp} (21830 cm^{-1}). The ligand-field strengths of these phosphines are nearly equal to those of en and tacn; the previously proposed Δ_{dmpe} value[5,14] seems to be too small. The more detailed spectroscopic analysis using the AOM treatment is now in progress.

The authors wish to thank Prof. Claus E. Schäffer (University of Copenhagen) for valuable discussions. The present work was supported in part by Grants-in-Aid for Scientific Research Nos. 09740489 and 11640562 from Ministry of Education, Science, Sports and Culture.

References

1 L. F. Larkworthy, K. B. Nolan, and P. O'Brien, "Comprehensive Coordination Chemistry," ed by G. Wilkinson, R. Gillard, and J. A. McCleverty, Pergamon, Oxford (1987), Vol. 3, Chapter 35.

2 L. F. Warren and M. A. Bennett, *Inorg. Chem.*, **15**, 3126 (1976).

3 R. D. Feltham and W. Silverthorn, *Inorg. Chem.*, **7**, 1154 (1968).

4 L. R. Gray, A. L. Hale, W. Levason, F. P. McCullough, and M. Webster, *J. Chem. Soc., Dalton Trans.*, **1983**, 2573; L. R. Gray, A. L. Hale, W. Levason, F. P. McCullough, and M. Webster, *J. Chem. Soc., Dalton Trans.*, **1984**, 47.

5 A. L. Hale and W. Levason, *J. Chem. Soc., Dalton Trans.*, **1983**, 2569.

6 J. E. Salt, G. Wilkinson, M. Motevalli, and M. B. Hursthouse, *J. Chem. Soc., Dalton Trans.*, **1986**, 1141.

7 A. M. Arif, J. G. Hafner, R. Jones, and B. R. Whittlesey, *Inorg. Chem.*, **25**, 1080 (1986).

8 F. A. Cotton and R. L. Luck, *Acta Crystallogr., Sect. C*, **47**, 1069 (1991).

9 F. A. Cotton, J. L. Eglin, R. L. Luck, and K.-A. Son, *Inorg. Chem.*, **29**, 1802 (1990).

10 F. R. Askham, A. W. Maverick, and G. G. Stanley, *Inorg. Chem.*, **26**, 3963 (1987).

11 A. M. Arif, R. Jones, and J. G. Hafner, *J. Crystallogr. Spectr. Res.*, **16**, 673 (1986).

12 E. G. Thaler, K. Folting, J. C. Huffman, and K. G. Caulton, *J. Organomet. Chem.*, **376**, 343 (1989).

13 T. G. Gardner and G. S. Girolami, *J. Chem. Soc., Chem. Commun.*, **1987**, 1758.

14 A. B. P. Lever, "Inorganic Electronic Spectroscopy," 2nd ed., Elsevier, Amsterdam (1984).

15 L. G. Vanquickenborne and A. Ceulemans, *Coord. Chem. Rev.*, **48**, 157 (1983); L. S. Forster, *Chem. Rev.*, **90**, 331 (1990).

16 T. Suzuki, K. Kashiwabara, N. Tsuji, and K. Tatsumi, *Inorg. Chem.*, **39**, 3938 (2000); M. Kita, K. Kashiwabara, J. Fujita, S. Kurachi, and S. Ohba, *Bull. Chem. Soc. Jpn.*, **66**, 3686 (1993).

17 T. Ohishi, K. Kashiwabara, and J. Fujita, *Bull. Chem. Soc. Jpn.*, **56**, 3441 (1983).

18 T. Ohishi, K. Kashiwabara, and J. Fujita, *Bull. Chem. Soc. Jpn.*, **60**, 575 (1987); T. Ohishi, K. Kashiwabara, and J. Fujita, *Bull. Chem. Soc. Jpn.*, **60**, 583 (1987).

19 K. Oguni, T. Ohishi, M. Kita, K. Kashiwabara, and J. Fujita, *Bull. Chem. Soc. Jpn.*, **62**, 588 (1989).

20 M. Kita, K. Kashiwabara, J. Fujita, H. Tanaka, and S. Ohba, *Bull. Chem. Soc. Jpn.*, **67**, 2457 (1994).

21 S. Iwatsuki, H. Kato, K. Obeyama, S. Funahashi, N. Koshino, K. Kashiwabara, T. Suzuki and H. D. Takagi, *Inorg. Chem. Commun.*, **3**, 501 (2000); T. Ando, M. Kita, K. Kashiwabara, J. Fujita, S. Kurachi, and S. Ohba, *Bull. Chem. Soc. Jpn.*, **65**, 2748 (1992).

22 K. Kashiwabara, M. Kita, J. Fujita, S. Kurachi, and S. Ohba, *Bull. Chem. Soc. Jpn.*, **67**, 2145 (1994).

23 S. A. Butter and J. Chatt, *Inorg. Synth.*, **15**, 185 (1974).

24 T. Suzuki, K. Isobe, and K. Kashiwabara, *J. Chem. Soc., Dalton Trans.*, **1995**, 3609.

25 T. Suzuki, K. Isobe, K. Kashiwabara, J. Fujita, and S. Kaizaki, *J. Chem. Soc., Dalton Trans.*, **1996**, 3779.

26 R. G. Hughes and C. S. Garner, *Inorg. Chem.*, **6**, 1519 (1967).

27 T. Suzuki, T. Imamura, and S. Kaizaki, *Acta Crystallogr., Sect. C*, **55**, 182 (1999).

28 Molecular Structure Corporation and Rigaku Co Ltd., TeXsan, Single crystal structure analysis software, Ver. 1.9, The Woodlands, TX, USA and Akishima, Tokyo, Japan, (1998).

29 G. M. Sheldrich, *Acta Crystallogr., Sect A*, **46**, 467 (1990).

30 E. Petersen, *Acta Chem. Scand.*, **24**, 3362 (1990).

31 K. Nakamoto, "Infrared and Raman Spectra of Inorganic and Coordination Compounds," 4th ed, John Wiley & Sons (1986).

32 D. Sandrini, M. T. Gandolfi, L. Moggi, and V. Balzani, *J. Am. Chem. Soc.*, **100**, 1463 (1970).

33 S. Kaizaki, J. Hidaka, and Y. Shimura, *Bull. Chem. Soc. Jpn.*, **48**, 902 (1975).

34 The average Co–P bond length in *trans*-$[CoCl_2(dmpe)_2]ClO_4$ is 2.259 Å (Ref. 20), while that in *trans*-$[CoCl_2(dmpp)_2]ClO_4$ is 2.289 Å (M. Kita and K. Kashiwabara, unpublished work).

35 B. N. Figgis and P. A. Reynolds, *J. Chem. Soc., Dalton Trans.*, **1987**, 1747.

36 J. Glerup, P. Mønsted, and C. E. Schäffer, *Inorg. Chem.*, **15**, 1399 (1976).

37 B. N. Figgis and M. A. Hitchman, "Ligand Field Theory and Its Applications," Wiley-VCH, New York (2000).

38 In this study the second-order perturbation effects are not considered. Thus, the parameters are estimated as follows: for octahedral complexes, $E(^4\mathrm{T}_2) = \Delta(\mathrm{d})$, $E(^4\mathrm{T}_1) = \Delta(\mathrm{d}) + 12B$, $E(^2\mathrm{T}_2) = 15B + 5C$; for tetragonal complexes, $E(\mathrm{a}^4\mathrm{E}) = \Delta(\mathrm{d}) - \frac{1}{4}\Delta(\mathrm{e}) - \frac{1}{3}\Delta(\mathrm{t}_2)$, $E(^4\mathrm{B}_2) = \Delta(\mathrm{d}) + \frac{1}{2}\Delta(\mathrm{e}) + \frac{2}{3}\Delta(\mathrm{t}_2)$, $E(^4\mathrm{A}_2) = \Delta(\mathrm{d}) - \frac{1}{2}\Delta(\mathrm{e}) + \frac{2}{3}\Delta(\mathrm{t}_2) + 12B$, $E(\mathrm{b}^4\mathrm{E}) = \Delta(\mathrm{d}) + \frac{1}{4}\Delta(\mathrm{e}) - \frac{1}{3}\Delta(\mathrm{t}_2) + 12B$.

39 A. D. Kirk and C. Namasivayam, *Inorg. Chem.*, **27**, 1095 (1988).

40 W. A. Baker, Jr., and M. G. Phillips, *Inorg. Chem.*, **5**, 1042 (1966).

41 L. Dubicki and P. Day, *Inorg. Chem.*, **10**, 2043 (1971).

42 The data from Ref. 41 give the set of parameters, $\Delta(\mathrm{d}) = 19400$, $\Delta(\mathrm{e}) = 3800$, $\Delta(\mathrm{t}_2) = 2250$ and $B = 533\ \mathrm{cm}^{-1}$ for *trans*-$[CrCl_2(en)_2]^+$, $\Delta(\mathrm{d}) = 18830$, $\Delta(\mathrm{e}) = 5300$, $\Delta(\mathrm{t}_2) = 1530$ and $B = 555\ \mathrm{cm}^{-1}$ for *trans*-$[CrBr_2(en)_2]^+$.

43 T. Schönherr, *Top. Curr. Chem.*, **191**, 88 (1997); D. W. Smith, *Struct. Bonding*, **35**, 87 (1978).

44 M. A. Bennett, R. J. H. Clark, and A. D. J. Goodwin, *Inorg. Chem.*, **6**, 1625 (1967).